RSC Advances

PAPER

View Article Online
View Journal | View Issue

Cite this: *RSC Adv.*, 2020, **10**, 37974

Selective oxidation of alcohols and sulfides *via* O_2 using a Co(II) salen complex catalyst immobilized on KCC-1: synthesis and kinetic study

Ali Allahresani, * Elaheh Naghdi, Mohammad Ali Nasseri and Kaveh Hemmat

The aim of this study was to immobilize a Co(II) salen complex on KCC-1 as a catalyst that can be recovered (Co(II) salen complex@KCC-1). Field-emission transmission electron microscopy, FT-IR spectroscopy, thermogravimetric analysis, elemental analysis, atomic absorption spectroscopy, and XRD were used to confirm the structure and chemical nature of Co(II) salen complex@KCC-1. The oxidation efficiency was obtained for an extensive range of sulfides and alcohols using this sustainable catalyst, alongside O_2 as an oxygen source and isobutyraldehyde (IBA) as an oxygen acceptor, with superior selectivity and conversion for the relevant oxidation products (sulfoxides and ketones or aldehydes) under moderate conditions. The μ-oxo and peroxo groups on the ligands of the Co complex appeared to be responsible for the superior activity of the catalyst. Essential factors behind the oxidation of alcohol and sulfoxides were investigated, including the catalyst, solvent, and temperature. In this paper, molecular oxygen (O_2) was used as a green oxidant. Furthermore, kinetic studies were conducted, revealing a first-order reaction for the oxidation of both benzyl alcohol and sulfide. The reaction progressed at mild temperature, and the catalyst could be easily recovered and reused for numerous consecutive runs under the reaction conditions, without any substantial reduction in the functionality of the catalytic system.

Received 9th August 2020
Accepted 14th September 2020

DOI: 10.1039/d0ra06863b

rsc.li/rsc-advances

Introduction

The simple separation and recovery of a catalyst is a significant area within green chemistry. It is complicated to separate reaction products from homogeneous catalysts; their immobilization on various supports is the most common way. Therefore, their catalytic performance can be improved by fixing metal complexes onto a solid support with a large surface area. Although some exciting features including the capability to be reused numerous times and stability against leaching can be obtained by heterogeneous catalysts,[1] procedures such as filtration, centrifugation and sedimentation are time-consuming, and separating the catalyst from the reaction environment can be ineffective. The performance of homogeneous catalysts is higher than that of heterogeneous catalysts. Thus, catalytic systems that exhibit the benefits of both heterogeneous and homogeneous catalysts are extremely important in modern chemistry.[2] The advantages of conventional catalysts include superior activity and improved stability.[3] For essential and challenging reactions, anchoring metal nanoparticles onto a solid support of choice offers an excellent opportunity for discovering novel, extremely active nanocatalysts. At the same time, the additional advantage of recyclability is also offered. Among the most significant study areas of advanced functional materials is surface-functionalized mesoporous materials. Polshettiwar *et al.*[4] reported fibrous nano-silica (KCC-1), with a large surface area and effortless access *via* its fibers (unlike the traditional usage of pores). For catalysts based on noble metals with superb catalytic efficiency and excellent availability of the active sites, KCC-1 would be an ideal catalyst support candidate.[4]

Metal nanocatalysts may be immobilized in two ways on the support. One method involves the deposition of presynthesized metal nanoparticles onto the support by chemical adsorption.[5] The precise control on the shape and size of the metal nanoparticles can be achieved by this approach, but the operation steps are tedious. During the catalytic reaction, the adsorbed nanocatalysts can also easily leach from the KCC-1 support. The other method involves the direct growth of metal nanoparticles on the KCC-1 support using grafted organic functional molecules or polymers as a stabilizer.[6] This procedure is superior for holding the metallic nanoparticles. Recently, chelating ligands of amine bis(phenol) have performed a significant role in the study of transition-metal catalysts,[7–9] in attempts to regulate the catalytic performance of the metal complexes. This exciting class of ligands contains the donor atoms O and N. Accordingly, the Lewis acidity of the metal centers can be tuned *via* various substituents on the phenol rings of these ligands. There have been several reports of catalysts containing these ligands coordinated to transition metals within model complexes of Co(II) and Co(III).[10–12]

Department of Chemistry, College of Sciences, University of Birjand, Birjand 97175-615, Iran. E-mail: a_allahresani@birjand.ac.ir

Since the oxidation of alcohols to ketones or aldehydes is a basic conversion in organic synthesis, the selective conversion of alcohols to the corresponding carbonyl compounds is among the most significant procedures.[13,14] To achieve these selective oxidation reactions, traditional methods include the usage of a stoichiometric amounts of oxidants such as chromium oxides[15] and manganese(IV) oxide,[16,17] which involves the production of vast quantities of poisonous waste. Catalytic oxidation procedures that use air or molecular oxygen are exciting and valuable, because of the increasing requirements for cost-effectiveness and environmental conservation.[18] In the literature, several methods based on metal catalysts and the aerobic oxidation of alcohols have been reported, including Au or Au/CuO-hydroxyapatite,[19,20] ruthenium,[21,22] cobalt,[23,24] and manganese nanoparticles.[25,26] The most widely reported methods involve catalytic systems dependent on NO radicals such as NHPI and TEMPO in combination with catalysts.[27–29] The use of aldehyde as a reducing factor in oxidation reactions has been broadly reported for the activation of dioxygen, with catalysts including Co salen complexes[30] and metalloporphyrins,[31] *etc.* The efficient oxidation of alcohol *via* isobutyraldehyde (IBA) and Cu(II) *meso*-tetraphenylporphyrin (TPP) has been reported by Rahimi *et al.*[32] An effective oxidation procedure of alcohol with IBA and O_2 using a ruthenium tetraphenylporphyrin (TPP) has also been reported.[33] Using IBA as a co-substrate, recently, an organic–inorganic hybrid cobalt phthalocyanine showed great efficiency for the oxidation of alcohols with high selectivity.[34] In efforts to improve catalysts for organic oxidation procedures, metal salen complexes have been studied intensively. The oxidation of olefins and sulfides by Fe_3O_4@SiO_2/Mn(III) chiral salen complex with H_2O_2 and TBHP, respectively, as oxidants,[35] and the selective oxidation of alcohols catalyzed *via* Co(III) salen complex with molecular oxygen as the oxidant,[36] have also been reported. Moreover, it has recently been reported[37–40] that in the preparation of biological and chemical molecules such as medications, the selective oxidation of sulfides to the corresponding sulfoxides *via* heterogeneous and homogeneous catalysts, is beneficial. In this process, the application of a green inorganic and organic oxidant are desirable, due to the waste resulting from most common oxidation reactions, which can be dangerous.

Recently, many reactions for the oxidation of alcohols and sulfides have been performed using cobalt salen complexes. For example, Vargas *et al.* showed phenol oxidation with a Co(II) salen complex catalyst supported on nanoporous materials *via* air,[41] and Nasseri *et al.* used $CoFe_2O_4$@SiO_2@-Co(III) salen complex nanoparticles for the oxidation of benzyl alcohols by molecular O_2.[36] Allahresani *et al.* applied a Co(III)@Fe_3O_4@SiO_2 salen complex as a highly selective and recoverable magnetic nanocatalyst for the oxidation of benzyl alcohols and sulfides.[42] The μ-oxo and peroxo groups bonded to the Co in the complex appear to be responsible for the superior activity of the catalyst. In this work, the aerobic oxidation of alcohols and sulfides catalyzed by Co(II) salen complex@KCC-1 in the presence of IBA was developed (Scheme 1) as an important part of a green oxidation procedure using O_2. For the oxidation of alcohols and sulfides, the catalyst system is effective, exhibiting high yields for carbonyl compounds under mild conditions.

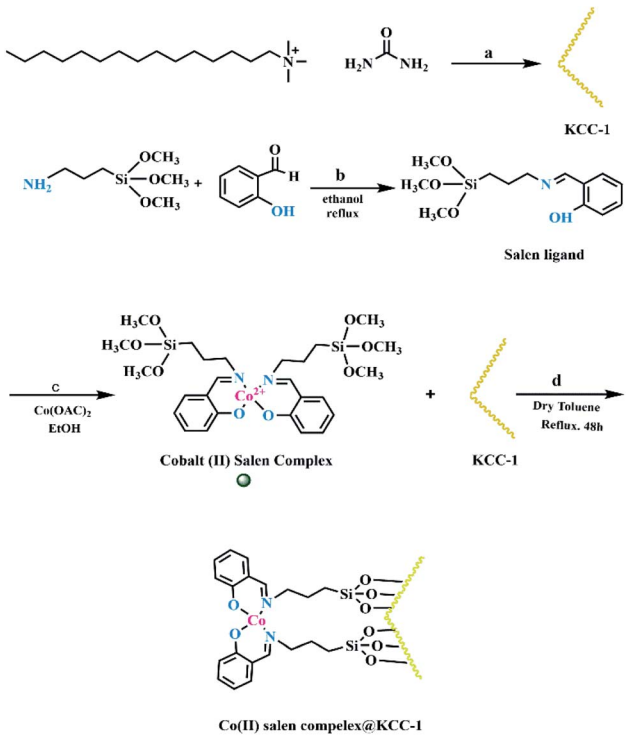

Scheme 1 Preparation of catalyst (Co(II) salen complex@KCC-1). Reagents and conditions: (a) TEOS, cyclohexane, 1-pentanol; (b) EtOH, reflux; (c) $Co(OAc)_2$, EtOH; (d) dry toluene, reflux, 48 h.

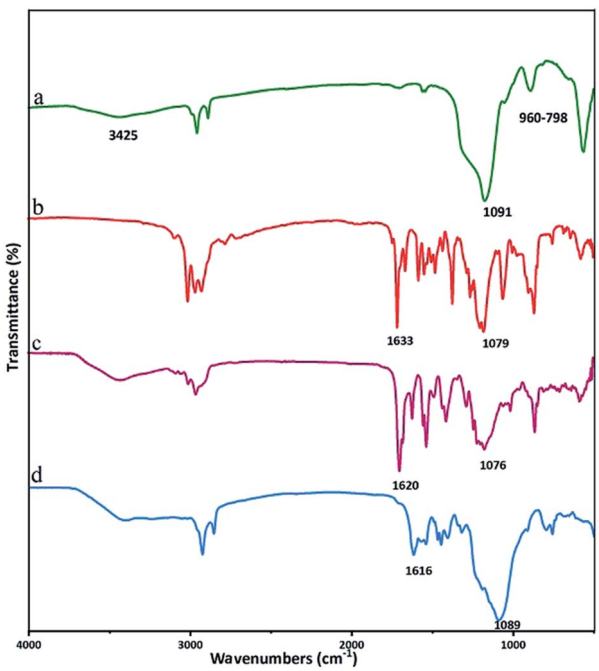

Fig. 1 FT-IR spectra of KCC-1 (a), salen ligand (b), Co(II) salen complex (c) and Co(II) salen complex@KCC-1 (d).

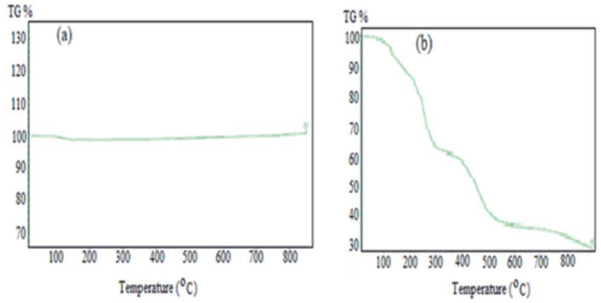

Fig. 2 TGA patterns of KCC-1 (a) and Co(II) salen complex@KCC-1 (b).

Results and discussion

Co(II) salen complex@KCC-1 was characterized using a vibrating sample magnetometer (VSM), Fourier transform infrared spectroscopy (FT-IR), transmission electron microscopy (TEM), energy dispersive X-ray (EDX) analyses, thermal gravimetric analysis (TGA), and powder X-ray diffractometry (XRD).

FT-IR spectroscopy

Fig. 1 presents infrared spectra of all components of Co(II) salen complex@KCC-1, which was synthesized in our lab. The KCC-1 spectrum (Fig. 1a) shows peaks at 1091, 915, and 805 cm^{-1}, attributed to Si–O and Si–OH, respectively. The peak at 3425 cm^{-1} is attributed to OH. The synthesis of KCC-1 was confirmed by the above vibrations.[7] Fig. 1b presents the infrared spectrum of the ligand, whose vibrations are in the zones of 1079 and 1633 cm^{-1}, which are attributed to Si and C=N, respectively.[43,44] Fig. 1c presents the infrared spectrum of the cobalt salen complex, in which the peaks at 1076 and 2923 cm^{-1} are attributed to Si and the methylene ring, respectively, while tensile vibrations of C=N are observed at 1620 cm^{-1}.[11,36] The peak at 1616 cm^{-1} appeared in the heterogeneous catalysts along with the peak 1089 cm^{-1} of Si–O–Si, confirming the successful fixation of the homogeneous cobalt complex on the KCC-1 surface (Fig. 1d).

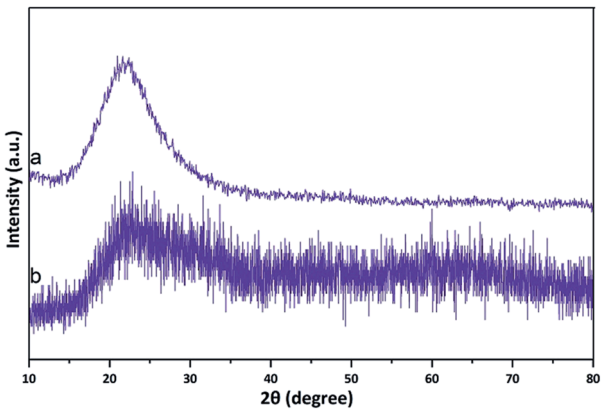

Fig. 3 XRD pattern of KCC-1 (a) and Co(II) salen complex@KCC-1 (b).

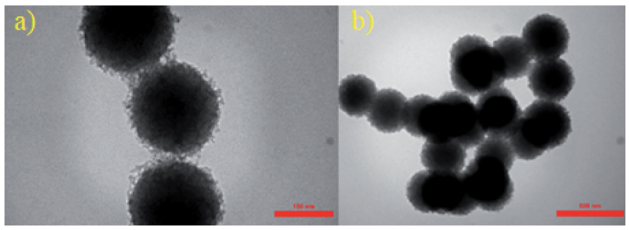

Fig. 4 TEM images of KCC-1 (a) and Co(II) salen complex@KCC-1 (b).

Thermal gravimetric analysis (TGA)

To assess the thermal stability of KCC-1 and Co(II) salen complex@KCC-1, TGA was carried out at temperatures ranging from ambient temperature to 850 °C (Fig. 2). Fig. 2a shows that the removal of H_2O occurred at temperatures below 130 °C (KCC-1). In Fig. 2b, water removal is the reason for the 4% weight loss in the range below 253 °C. The weight loss of about 10% in the temperature range of 250–450 °C was attributed to the removal of oxygen from the functional groups of the Co(II) salen complex and the 15% weight loss in the temperature range of 450–700 °C could be carbon removal. There was no additional weight loss above 700 °C and the total weight loss of the organic sections was evaluated to be 29% (see Fig. 2).

XRD analysis

XRD was used to investigate KCC-1 and Co(II) salen complex@KCC-1 (Fig. 3). KCC-1 is a dendritic nanosilica fibrous scaffold, and represents an important discovery due to its unique fibrous morphology. The complex was distributed uniformly in all directions, and the sample consisted of particles with uniform size (Fig. 3a). In Fig. 3b, the peak at $2\theta = 20–30°$ is attributed to amorphous silica. The structural similarity was confirmed by the comparison of the nanostructure pattern with that of the desired sample of this complex. Due to the similarity of the peaks, the structures of the complex and the nanostructure are the same and exist in an amorphous state. The width of the pattern is different simply because of the small size of the particles.

Transmission electron microscopy (TEM)

TEM images of KCC-1 and Co(II) salen complex@KCC-1 are shown in Fig. 4a and b, respectively. As the images show, the nanoparticles are spherical.

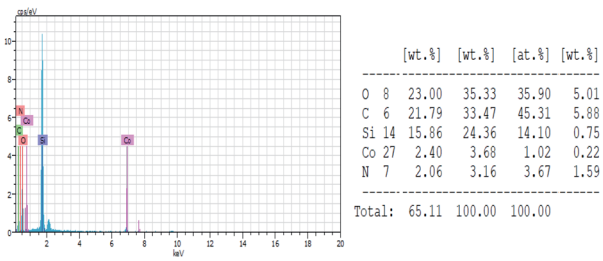

Fig. 5 Energy dispersive X-ray (EDX) of Co(II) salen complex@KCC-1.

Energy dispersive X-ray (EDX)

The Si, Co, O, N, and C composition of Co(II) salen complex@KCC-1 was confirmed using EDX elemental analysis. The coordination of cobalt with the Schiff-base of the mesoporous support is suggested by the peaks shown in Fig. 5.

Catalytic performance of Co(II) salen complex@KCC-1 for the aerobic oxidation of sulfides and alcohols

The catalytic performance of Co(II) salen complex@KCC-1 for benzyl alcohol (BzOH) aerobic oxidation to benzaldehyde (BzH) and sulfide (–S–) to sulfoxide (–SO–) was investigated for the first time. The optimum test conditions were determined by carrying out reactions at 60 °C, with dichloromethane (DCM), ethanol (EtOH), acetic acid (HOAc), acetonitrile (CH_3CN), and water as solvents, IBA as an oxygen acceptor, and Co(II) salen complex@KCC-1 as a catalyst (see Table 1, entries 1–7). The results show that the oxidation in acetic acid (HOAc) solution was more efficient than other solvents under the same conditions. However, there was no substantial oxidation reaction of water or ethanol (see Table 1, entries 1 and 2). Conversion by 20% could be obtained after 100 min of reaction with dichloromethane (DCM) and chloroform as solvents (see Table 1, entries 5 and 6). Moreover, the oxidation reaction efficiency was increased in an acidic environment. Acetic acid is a useful solvent that has been applied in the aerobic oxidation of alcohols and sulfides. It has previously been reported that acidic conditions can activate catalysts and increase oxygen consumption.[45]

It has been reported that aldehydes (RCHO) should be utilized to activate O_2. This means that IBA is significant in the aerobic oxidation method, and without it, the reaction would instantly cease (see Table 1, entry 14). In the current process, this suggests that the oxidation procedure takes place through a free-radical mechanism. Also, in the presence of 2,6-di-*tert*-butyl-4-methylphenol as a radical scavenger, a delay in the oxidation of benzyl alcohol also supports this claim. The optimized quantity of IBA was defined as 3 mmol. Due to the reduction in the amount of catalyst, significantly lower conversions were predictable (see Table 1, entries 8–10). The optimal result was obtained by using 0.06 g of Co(II) salen complex@KCC-1 and 3 mmol of IBA in 5 mL of acetic acid at 60 °C (see Table 1, entry 8).

Afterward, the efficacy of Co(II) salen complex@KCC-1 was determined for other benzylic alcohols (see Table 2).

Then, the efficiency of the catalyst was determined for other sulfides (see Table 3). In the present system, the transformation of several sulfides to the corresponding sulfoxides occurred with high conversion.

Molecular oxygen was utilized as an oxidant in this heterogenous reaction system. In the O_2 system, a hot filtration test

Table 1 The effect of diverse reaction conditions on the oxidation of benzyl alcohol with O_2/IBA as the oxygen donor/acceptor in the presence of Co(II) salen complex@KCC-1. Reaction conditions: IBA (*X* mmol), benzyl alcohol or sulfide (1 mmol), IBA[b] (3 mmol), O_2[c] (5 mL min^{-1}), Co(II) salen complex@KCC-1[a] (*Y* g)

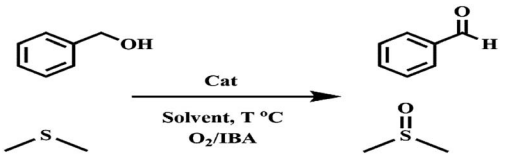

Entry	Cat[a] (g)	*T* (°C)	IBA[b] (mmol)	Solvent (mL)	*t* (min)	Conversion (%)
1	0.06	60	3	H_2O (5)	90	30
2	0.06	60	3	EtOH (5)	45	35
3	0.06	60	3	EtOAc (5)	120	70
4	0.06	60	3	CH_3CN (5)	35	85
5	0.06	60	3	CH_2Cl_2 (5)	100	20
6	0.06	60	3	$CHCl_3$ (5)	100	20
7	0.06	60	3	HOAc (5)	30	95
8	—	60	3	HOAc (5)	180	10
9	0.03	60	3	HOAc (5)	30	50
10	0.04	60	3	HOAc (5)	30	55
11	0.07	60	3	HOAc (5)	30	70
12	0.06	RT	3	HOAc (5)	180	55
13	0.06	80	3	HOAc (5)	180	45
14	0.06	60	—	HOAc (5)	30	40
15	0.06	60	1	HOAc (5)	30	58
16	0.06	60	2	HOAc (5)	30	64
17	0.06	60	4	HOAc (5)	30	70

[a] Co(II) salen complex@KCC-1 as the catalyst. [b] IBA as co-substrate. [c] O_2 as oxidant.

Table 2 Various benzyl alcohol oxidation reactions with O_2/IBA as the oxygen donor/acceptor in the presence of Co(II) salen complex@KCC-1[a] in HOAc. Reaction conditions: benzyl alcohol (1 mmol), IBA[b] (3 mmol), O_2[c] (5 mL min^{-1}), in 5 mL HOAc at 60 °C, 0.06 g of Co(II) salen complex@KCC-1[a]

Entry	Substrate	Product	*t* (min)	Conversion (%)	Selectivity (%)
1			30	95	99
2			30	85	92
3			30	68	90
4	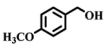		30	30	98
5			30	60	98
6			30	45	93
7			30	80	93
8			30	68	98
9			30	90	98

[a] Co(II) salen complex@KCC-1 as a catalyst. [b] IBA as co-substrate. [c] O_2 as oxidant.

Table 3 Oxidation of various sulfides with O_2/IBA as the oxygen donor/acceptor in the presence of Co(II) salen complex@KCC-1[a] in HOAc. Reaction conditions: sulfide (1 mmol), IBA[b] (3 mmol), O_2[c] (5 mL min^{-1}), in 5 mL HOAc at 60 °C, 0.06 g of Co(II) salen complex@KCC-1[a]

Entry	Substrate	Product	t (min)	Conversion (%)	Selectivity (%)
1			30	82	99
2			30	90	99
3			30	97	98
4			30	94	98
5			30	80	97

[a] Co(II) salen complex@KCC-1 as a catalyst. [b] IBA as co-substrate. [c] O_2 as oxidant.

was used to characterize the nature of the heterogeneous catalyst. As a model reaction, the aerobic oxidation reaction of sulfide and benzyl alcohol using Co(II) salen complex@KCC-1 in acetic acid was performed (Scheme 2). To remove the catalyst, filtration was used, achieving a conversion of 50%. Afterward, the filtrate was allowed to carry on reacting under the optimal reaction conditions. After 4 h, there was no substantial increase in the conversion. In this catalytic system, the high stability of the catalyst and its heterogeneous nature were confirmed *via* the hot filtration approach.

Possible mechanism

It has been reported that the activation of molecular oxygen *via* aldehydes occurs through a procedure involving free radicals. 2,6-Di-*tert*-butylphenol was utilized as an inhibitor of free-radical oxidation to verify the free-radical mechanism. The oxidation reaction was quenched when this inhibitor was added.

It has been reported by Beller that oxo ruthenium complexes are effective catalysts for the asymmetric oxidation of alkenes.[46]

The mechanism of the reaction can include the contribution of Co-oxo species resulting in a reaction between O_2 and Co(II)

Scheme 2 Oxidation of benzyl alcohol and sulfide by Co(II) salen complex@KCC-1.

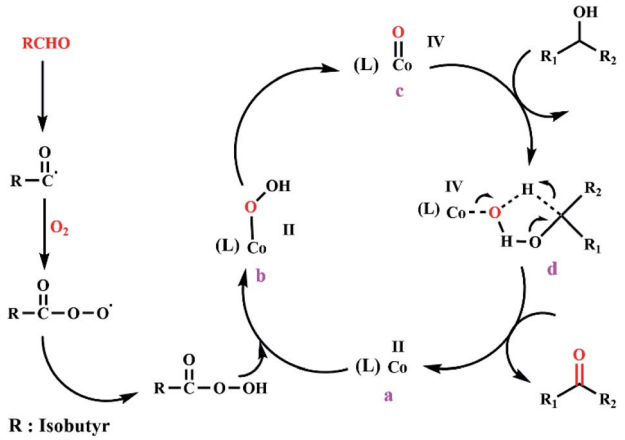

Scheme 3 An acceptable mechanism for Co(II) salen complex@KCC-1 catalyzing the oxidation of alcohol using IBA and O_2.

salen complex@KCC-1 *via* a series of radical chains in the presence of IBA. The production of carbonyl compounds corresponds to the reaction of Co-oxo species *via* alcohol, followed by the elimination of β-hydride. Based on the explanation given, in the presence of O_2 and IBA, an acceptable mechanism for benzyl alcohol oxidation catalyzed *via* Co(II) salen complex@KCC-1 is presented in Scheme 3.

Firstly, an acyl radical is derived from thermal hydrogen abstraction at the carbonyl position. Radical propagation occurs to generate peroxyacid. Then, the smooth interaction among peroxy acid and Co(II) salen complex (a) should initiate the reaction to produce Co(II)–OOH (b).[47,48] Then, Co-oxo (c) is formed from the heterolytic cleavage of the O–O bond of species (b). The production of a carbonyl compound corresponds to the reaction of the Co-oxo species with alcohol *via* a transition species (d), because of the electrophilic character of Co-oxo (c) followed by β-hydride elimination.[49,50]

Kinetic study

To investigate the kinetic data of the proposed nanocatalyst, pseudo-first and second-order models were studied.

The following first-order model (eqn (1)) was employed with integration conditions of $C_0 = 0.2$ M to $C = C_t$ at $t = 0$ to $t = t$, expressed as eqn (2).

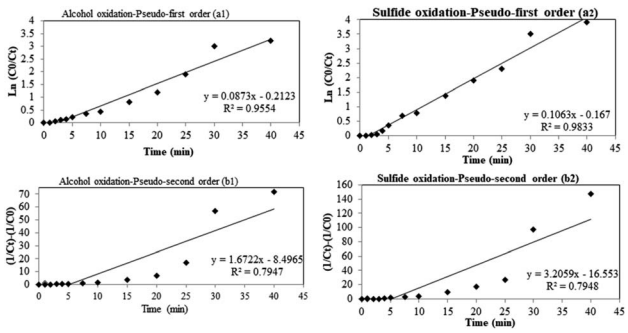

Fig. 6 Alcohol oxidation-pseudo-first order (a1) and sulfide oxidation pseudo-first order (a2); alcohol oxidation-pseudo-first order (b1) and sulfide oxidation-pseudo-first order (b2).

$$dC/dt = k_1(C_0 - C_t) \quad (1)$$

$$\ln(C_0/C_t) = k_1 t \quad (2)$$

The first-order rate constant k_1 can be obtained from the slope of the $\ln(C_0/C_t)$ *versus* t plot illustrated in Fig. 6a. k_1 was found to be 0.0873 and 0.1063 min^{-1} for the oxidation of benzyl alcohols and sulfides, respectively. On the other hand, the pseudo-second-order model given as follows (eqn (3)), was integrated for the above boundary conditions, which are simplified in eqn (4).

$$dC/dt = k_2(C_0 - C_t)^2 \quad (3)$$

$$1/C_t - 1/C_0 = k_2 t \quad (4)$$

k_2 (mL $mmol^{-1}$ min^{-1}) is the rate constant of the second-order model, which can be determined by plotting $1/C_t - 1/C_0$ *versus* t. k_2 values of 1.6722 and 1.3069 were obtained for the oxidation of benzyl alcohols and sulfides, respectively. Also, Fig. 6b shows that the correlation coefficient values of the pseudo-first-order model were higher than those of the pseudo-second-order model for both benzyl alcohols and sulfides, suggesting that the oxidation procedure using the proposed nanocatalyst follows first-order kinetics.

Recycling of the catalyst

The ability to reuse a catalyst is very important both economically and practically. Thus, the reusability of Co(II) salen complex@KCC-1 for the alcohol and sulfide oxidation reactions was investigated in the O_2 system under the optimized conditions. In each run, centrifugation was applied to recover the catalyst after 30 minutes. At 60 °C, it was reused after washing with ethanol and drying. In the case of the O_2 system, Co(II) salen complex@KCC-1 showed high catalytic performance for at least five runs (see Fig. 7 and 8).

Next, we compared the present results with some previously reported data to evaluate the catalytic efficiency and reusability of Co(II) salen complex@KCC-1 for aerobic epoxidation of olefins with molecular oxygen (Table 4).

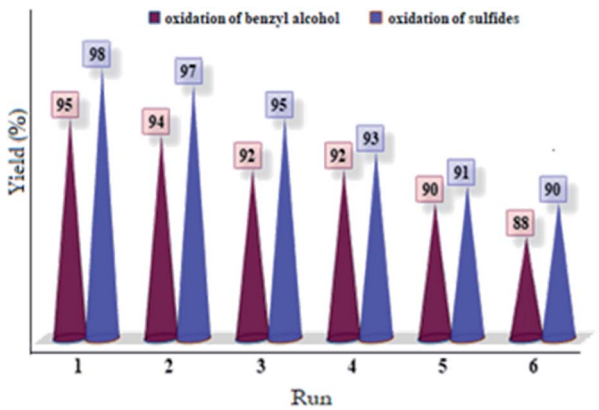

Fig. 7 Recyclability of Co(II) salen complex@KCC-1 in the oxidation of benzyl alcohol and sulfides.

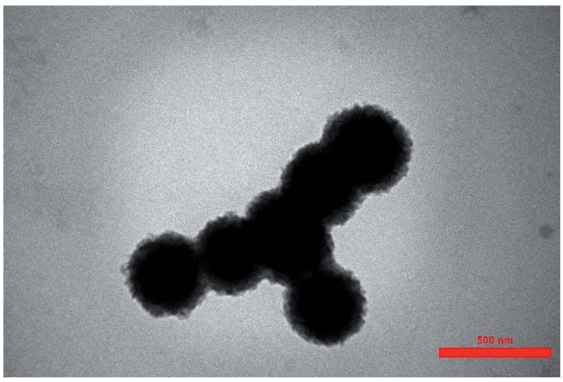

Fig. 8 TEM image of the recycled catalyst.

Experimental

Synthesis of KCC-1

KCC-1 was prepared using a microwave-assisted hydrothermal technique. CTAB (cetyltrimethylammonium bromide, 2 g, 5.48 mmol) and urea (2.4 g, 40 mmol) were stirred (1500 RPM) in water (300 mL) for 15 min. TEOS (tetraethyl orthosilicate, 10 mL) was taken in cyclohexane (100 mL) and added dropwise to the above solution, and the solution was stirred further for 15 min, followed by the dropwise addition of 1-pentanol (6 mL, 55.2 mmol). The resultant solution was stirred for 30 min at room temperature. Then the reaction mixture was transferred into a Teflon-sealed 1 L microwave (MW) reactor, at 120 °C, and irradiated (800 W power) for 4 h under moderate stirring. After completion of the reaction, the solid product was isolated by centrifugation, washed several times with water and ethanol, and dried at 80 °C for 8 h. The as-synthesized material was then calcined at a rate of 2.5 °C min^{-1} at 550 °C for 6 h in the air to yield calcined fibrous nano-silica (KCC-1).

Synthesis of salen ligand

The Schiff base was prepared as follows. 3-Aminopropyltrimethoxysilane (1.2 mmol) was added to a mixture of 2-hydroxybenzaldehyde (1.0 mmol) in ethanol (10 mL) and stirred under reflux conditions for 3 h. The color of the reaction solution changed to yellowish, due to imine formation, and the solvent of mixture was eliminated at 70 °C, to obtain an oily product.

Synthesis of Co(II) salen complex

Functionalized salen ligand (1.0 mmol) was dissolved in ethanol (20 mL). Then NaOH (1.67 mmol) and Co(II) acetate monohydrate (1 mmol) were added and the reaction was refluxed under argon gas for 3 h. The reaction mixture was cooled to 0 °C and the precipitate was filtered. The precipitate was washed with methanol, water, and diethyl ether, in sequence, to purify it. Dark green sediment formed following drying at 80 °C in an oven under vacuum.

Synthesis of Co(II) salen complex@KCC-1

The Co(II) salen complex@KCC-1 nanocatalyst was synthesized according to the following procedure: KCC-1 (0.25 g) was

Table 4 Comparison of results using Co(II) salen complex@KCC-1 with various catalysts[a]

Entry	Catalyst	Oxidant	Solvent	Yield (%)	Ref.
1	Ni(II)DPDME	O_2/IBA	CH_3CN	33	50
2	Mn_6Ni_4	O_2	Toluene	89	51
3	Co–Ni ferrite	TBHP/*hv*	CH_3CN	18.9	52
4	Fe (THPP)Cl@MWCNT	O_2/IBA	DMF	89	53
5	$Rd_2(OAc)_4$	O_2/iPrCHO	Acetone	88	54
6	CoO–MCM-41	O_2/IBA	1,2-Dichloroethane	90	55
7	Co(II) salen complex@KCC-1	O_2/IBA	HOAc	95	This work

[a] Reaction conditions: benzyl alcohol (1 mmol), IBA[b] (3 mmol), O_2[c] (5 mL min^{-1}), in 5 mL HOAc at 60 °C, and 0.06 gram of Co(II) salen complex@KCC-1.

dispersed in 30 mL of dry toluene for 30 min. Then, 0.7 g of homogeneous Co(II) salen complex was added into the suspension. After refluxing for 20 h, the immobilized catalyst was filtered and the precipitate was washed 3 times with dry toluene, 3 times with ethanol, and 3 times with dichloromethane. Then, the solid mixture was dried at 80 °C under vacuum for 8 h.

General procedure for the oxidation of alcohol

For the aerobic oxidation of alcohols, 0.06 g of Co(II) salen complex@KCC-1, 1 mmol alcohol, 3 mmol IBA and 5 mL of acetic acid were added to a 10 mL flask, which was placed under oxygen gas conditions. At 60 °C, the mixture was stirred for 30 min. Through the reaction, dioxygen was bubbled at a rate of 5 mL min^{-1}. The reaction was monitored using TLC on silica gel.

General procedure for the oxidation of sulfide

For the aerobic oxidation of sulfide, 0.06 g of Co(II) salen complex@KCC-1, 1 mmol sulfide, 3 mmol IBA (IBA) and 5 mL of acetic acid were added to a 10 mL flask, which was placed under oxygen gas conditions. At 60 °C, the mixture was stirred for 30 min. Throughout the reaction, dioxygen was bubbled at a rate of 5 mL min^{-1}. The reaction was monitored using TLC on silica gel.

Conclusions

In brief, in the presence of molecular oxygen and IBA, Co(II) salen complex@KCC-1 has been shown to be an excellent catalyst for the oxidation of sulfides and alcohols. The chemical properties and structural stability of the catalyst were confirmed. We demonstrated that the eco-friendly system provides a novel and precise catalyst for the oxidation of a broad range of sulfides and alcohols into the corresponding sulfoxides and aldehydes/ketones under green and moderate conditions. Because Co is widely available and inexpensive, this catalyst can be discovered, easily. Also, our catalyst can overcome the current problem in the oxidation of sulfides: over-oxidation of sulfoxides to the relevant sulfones. The effects of different reaction parameters, including catalyst, solvent, and temperature were evaluated on the selectivity and activity. Moreover, the catalyst was reused in alcohol and sulfide oxidation reactions for five successive cycles.

Conflicts of interest

The authors declare no conflict of interest.

Acknowledgements

The authors are grateful to the University of Birjand for financial support.

References

1 Q. H. Xia, H. Q. Ge, C. P. Ye, Z. M. Liu and K. X. Su, *Chem. Rev.*, 2005, **105**, 1603–1662.
2 Z. X. Li, W. Xue, B. T. Guan, F. B. Shi, Z. J. Shi, H. Jiang and C. H. Yan, *Nanoscale*, 2013, **5**, 1213–1220.
3 S. M. Sadeghzadeh, *Catal. Sci. Technol.*, 2016, **6**, 1435–1441.
4 V. Polshettiwar, D. Cha, X. Zhang and J. M. Basset, *Angew. Chem., Int. Ed.*, 2010, **49**, 9652–9656.
5 J. P. Ge, T. Huynh, Y. P. Hu and Y. D. Yin, *Nano Lett.*, 2008, **8**, 931–934.
6 S. M. Sadeghzadeh, R. Zhiani and S. Emrani, *RSC Adv.*, 2017, **7**, 24885–24894.
7 A. K. Bowser, A. M. Anderson-Wile, D. H. Johnston and B. M. Wile, *Appl. Organomet. Chem.*, 2016, **30**, 32–39.
8 E. Safaei, L. Hajikhanmirzaei, B. Karimi, A. Wojtczak, P. Cotič and Y.-I. Lee, *Polyhedron*, 2016, **106**, 153–162.
9 S. Yang, K. Nie, Y. Zhang, M. Xue, Y. Yao and Q. Shen, *Inorg. Chem.*, 2014, **53**, 105–115.
10 M. A. Nasseri, K. Hemmat and A. Allahresani, *Appl. Organomet. Chem.*, 2019, **33**, e4743.
11 K. Hemmat, M. A. Nasseri and A. Allahresani, *ChemistrySelect*, 2019, **4**, 4339–4346.
12 M. A. Nasseri and A. Allahresani, *J. Chem. Sci.*, 2017, **129**, 343–352.
13 R. H. Crabtree, *Chem. Rev.*, 2017, **117**, 9228–9246.
14 H. Su, K. X. Zhang, B. Zhang, H. H. Wang, Q. Y. Yu, X. H. Li, M. Antonietti and J. S. Chen, *J. Am. Chem. Soc.*, 2017, **139**, 811–818.
15 C. B. Wang, Y. P. Cai and I. E. Wachs, *Langmuir*, 1999, **15**, 1223–1235.

16 O. Delacroix, B. Andriamihaja, S. Picart-Goetgheluck and J. Brocard, *Tetrahedron*, 2004, **60**, 1549–1556.
17 R. Ziessel, P. Nguyen, L. Douce, M. Cesario and C. Estournes, *Org. Lett.*, 2004, **6**, 2865–2868.
18 T. Mallat and A. Baiker, *Chem. Rev.*, 2004, **104**, 3037–3058.
19 L. Wang, X. J. Meng, B. Wang, W. Y. Chi and F. S. Xiao, *Chem. Commun.*, 2010, **46**, 5003–5005.
20 T. Tian, Y. Liu and X. Zhang, *Chin. J. Catal.*, 2015, **36**, 1358–1364.
21 R. Ray, S. Chandra, D. Maiti and G. K. Lahiri, *Chem.–Eur. J.*, 2016, **22**, 8814–8822.
22 Z. Hao, X. Yan, Z. Li, R. Wu, Z. Ma, S. Li, Z. Han, X. Zheng and J. Lin, *Transition Met. Chem.*, 2018, **43**, 635–640.
23 Y. B. Kuang, Y. Nabae, T. Hayakawa and M. Kakimoto, *Appl. Catal., A*, 2012, **423**, 52–58.
24 A. Shaabani, S. Keshipour, M. Hamidzad and S. Shaabani, *J. Mol. Catal. A: Chem.*, 2014, **395**, 494–499.
25 G. Elmaci, D. Ozer and B. Zumreoglu-Karan, *Catal. Commun.*, 2017, **89**, 56–59.
26 G. Wu, Y. Gao, F. W. Ma, B. H. Zheng, L. G. Liu, H. Y. Sun and W. Wu, *Chem. Eng. J.*, 2015, **271**, 14–22.
27 F. Rajabi and B. Karimi, *J. Mol. Catal. A: Chem.*, 2005, **232**, 95–99.
28 J. M. Hoover, B. L. Ryland and S. S. Stahl, *ACS Catal.*, 2013, **3**, 2599–2605.
29 Y. T. Yan, X. L. Tong, K. X. Wang and X. Q. Bai, *Catal. Commun.*, 2014, **43**, 112–115.
30 Z. F. Li, S. J. Wu, H. Ding, D. F. Zheng, J. Hu, X. Wang, Q. S. Huo, J. Q. Guan and Q. B. Kan, *New J. Chem.*, 2013, **37**, 1561–1568.
31 S. Y. Chen, X. T. Zhou and H. B. Ji, *Catal. Today*, 2016, **264**, 191–197.
32 R. Rahimi, E. Gholamrezapor and M. R. Naimi-jamal, *Inorg. Chem. Commun.*, 2011, **14**, 1561–1568.
33 H. B. Ji, Q. L. Yuan, X. T. Zhou, L. X. Pei and L. F. Wang, *Bioorg. Med. Chem. Lett.*, 2007, **17**, 6364–6368.
34 V. Panwar, P. Kumar, S. S. Ray and S. L. Jain, *Tetrahedron Lett.*, 2015, **5**, 3948–3953.
35 A. Allahresani and M. A. Nasseri, *RSC Adv.*, 2014, **4**, 60702–60710.
36 M. A. Nasseri, K. Hemmat, A. Allahresani and E. Hamidi-Hajiabadi, *Appl. Organomet. Chem.*, 2019, **33**, e4809.
37 B. Li, S. Bai, P. Wang, H. Yang, Q. Yang and C. Li, *Phys. Chem. Chem. Phys.*, 2011, **13**, 2504–2511.
38 B. Li, A.-H. Liu, L.-N. He, Z.-Z. Yang, J. Gao and K.-H. Chen, *Green Chem.*, 2012, **14**, 130–135.
39 Z. Yang, C. Zhu, Z. Li, Y. Liu, G. Liu and Y. Cui, *Chem. Commun.*, 2014, **50**, 8775–8778.
40 W. Zhao, C. Yang, Z. Cheng and Z. Zhang, *Green Chem.*, 2016, **18**, 995–998.
41 D. X. M. Vargas, J. R. De La Rosa, S. A. Iyoob, C. J. Lucio-Ortiz, F. J. C. Córdoba and C. D. Garcia, *Appl. Catal., A*, 2015, **506**, 44–56.
42 A. Allahresani, M. A. Nasseri, A. Nakhaei and S. Aghajani, *Iran. Chem. Commun.*, 2019, **7**, 153–169.
43 K. Hemmat, M. A. Nasseri and A. Allahresani, *Appl. Organomet. Chem.*, 2019, **33**, e4937.
44 E. Vinck, D. M. Murphy, I. A. Fallis, R. R. Strevens and S. V. Doorslaer, *Inorg. Chem.*, 2010, **49**, 2083–2092.
45 R. Malakooti and A. Feghhi, *New J. Chem.*, 2017, **41**, 3405–3413.
46 M. K. Tse, S. Bhor, M. Klawonn, C. Dobler and M. Beller, *Tetrahedron Lett.*, 2003, **44**, 7479–7483.
47 M. Bar, S. Deb, A. Paul and S. Baitalik, *Inorg. Chem.*, 2018, **57**, 12010–12024.
48 J. L. Pratihar, P. Pattanayak, J. H. Huang and S. Chattopadhyay, *Inorg. Chim. Acta*, 2009, **362**, 5170–5174.
49 Q. Han, X. X. Guo, X. T. Zhou and H. B. Ji, *Inorg. Chem. Commun.*, 2020, **112**, 107544.
50 C. Sun, B. Hu and Z. Liu, *Heteroat. Chem.*, 2012, **23**, 295–303.
51 Q. Tang, C. Wu, R. Qiao, Y. Chen and Y. Yang, *Appl. Catal., A*, 2011, **403**, 136–141.
52 J. Tong, Q. Zhang, L. Bo, L. Su and Q. Wang, *J. Sol-Gel Sci. Technol.*, 2015, **76**, 19–26.
53 M. J. Beier, W. Kleist, M. T. Wharmby, R. Kissner, B. Kimmerle, P. A. Wright and A. Baiker, *Chem.–Eur. J.*, 2012, **18**, 887.
54 D. Shabashov and M. P. Doyle, *Tetrahedron*, 2013, **69**, 10009–10013.
55 D. Dhar, Y. Koltypin, A. Gedanken and S. Chandrasekaran, *Catal. Lett.*, 2003, **86**, 197–200.